Confinement Studies of Auxiliary Heated NSTX Plasmas

B.P. LeBlanc 1), M.G. Bell 1), R.E. Bell 1), C. Bourdelle 2), C.E. Bush 3), D.A. Gates 1), J.C. Hosea 1), D.W. Johnson 1), S.M. Kaye 1), R. Maingi 1), J.E. Menard 1), D. Mueller 1), M. Ono 1), S.F. Paul 1), M. Peng 3) , A.L. Roquemore 1), S.A. Sabbagh 4), D. Stutman 5), E.J. Synakowski 1), V.A. Soukhanovskii 1), J.R.Wilson 1) and the NSTX Research Team

1) Princeton Plasma Physics Laboratory, Princeton University, Princeton, New Jersey 08543
2) DRFC, CEA, Cadarache, Saint-Paul lez Durance cedex, France
3) Oak Ridge National Laboratory, Oak Ridge, Tennessee 37830
4) Department of Applied Physics, Columbia University New York, New York 10027
5) Johns Hopkins University, Baltimore, Maryland

e-mail contact of main author: bleblanc@pppl.gov

Abstract: The confinement of auxiliary heated NSTX discharges is discussed. The energy confinement time (in plasmas with either L-mode or H-mode edges) scales favorably compared to ITER97L and ITRE98Pby(2) scalings, being up to 2-3 times L-mode and 1.5 time H-mode. TRANSP calculations based on the kinetic profile data reproduce the magnetics-based determination of stored energy and the measured neutron production rate. Power balance calculations reveal ion thermal transport to be near neoclassical level, and well below the electron thermal transport, which is the main loss channel. Perturbative impurity injection techniques also indicate the particle diffusivity to be near the neoclassical level. H-mode operation has been obtained during high-harmonic fast-wave heating.

1. Introduction

The National Spherical Torus Experiment (NSTX) is a medium size toroidal magnetic confinement device using the spherical torus (ST) geometry [1], which combines the advantages of plasma shaping with an intrinsic strong magnetic shear associated with low aspect ratio. The device has a large plasma with nominal plasma parameters of geometrical center major radius of 0.85 cm and minor radius 0.68 m, giving an aspect ratio of ≥ 1.27. The toroidal field covers an operational range of 0.3-0.6 T, and discharges with plasma currents up to 1.5 MA have been produced. The device can operate in inner-wall limited, single-null or double-null configurations, producing shaped plasmas with elongation $\kappa \leq 2.2$, and triangularly $\delta \leq 0.8$. So far NSTX has achieved, non-simultaneously, stored energies up to 0.39 MJ, energy confinement times $\tau_E < 0.12$ s and $\beta_T \leq 34\%$ [2], where β_T is defined as $\langle p \rangle / (B_0^2/2\mu_0)$, where $\langle p \rangle$ is the volume averaged total pressure and B_0 is the vacuum magnetic field at the geometric center. Auxiliary heating plays an important

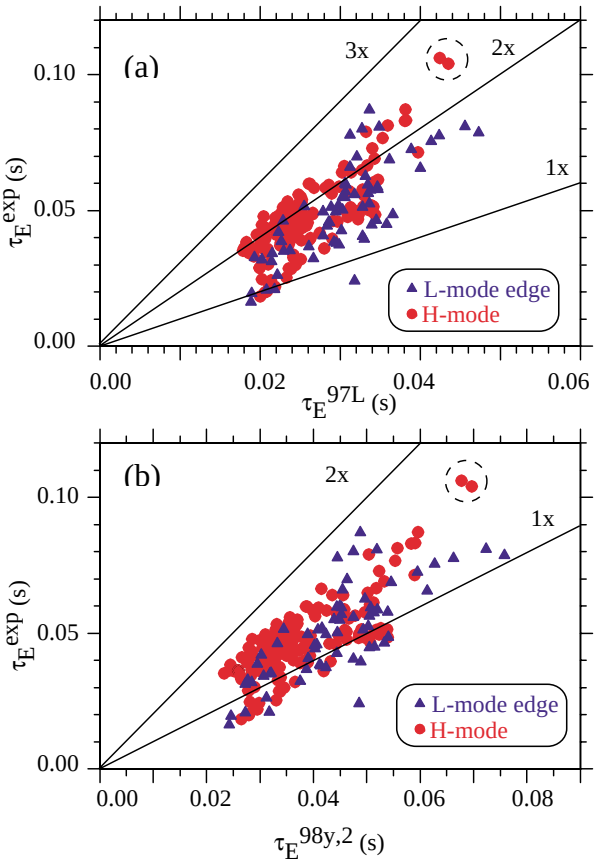

FIG.1: Energy confinement against ITER database scalings ITER97L (a) and ITER98Pby(2) (b). Discharges in dashed circles are transient.

role in the research program, with deuterium neutral beam injection (NBI) powers of up to 7 MW at injection energies up to 100 keV, and high-harmonic fast-wave (HHFW) heating with powers up to 6 MW. A recent machine upgrade permits baking at 350° C, supplementing boronization [3] and helium glow to condition the first-wall surfaces.

This paper discusses confinement during auxiliary heating. We begin with a comparison of the global energy confinement time against ITER database scalings. We continue with a description of the kinetic profile data set presently implemented and discuss its utilization within the data analysis code TRANSP. The present understanding of the different local transport coefficients is discussed. The last section discusses the HHFW driven H-mode discharges. We close with conclusions and future plans.

2. Global Confinement Scaling

The global confinement in NSTX is remarkably good, easily comparable to that of tokamaks of similar size whose toroidal fields are significantly larger. In Fig. 1(a) is shown the experimental energy confinement time plotted against the value determined from the L-mode scaling ITER97L [4]. The experimental energy confinement times were determined from the EFIT magnetic reconstructions of the NSTX plasmas. Except for the two plasmas indicated by dashed circles, the discharges shown have achieved a non-transient phase lasting at least two confinement times. H-mode plasmas are indicated by red circles, while L-mode edge plasmas are shown with blue triangles. In Fig. 1(b) we present a similar plot for the ITER98Pby(2) [5] H-mode scaling. It is seen that the L-mode edge plasmas in NSTX can achieve comparatively good or equivalent confinement as the H-mode plasmas. The NSTX data lay above both scalings, being up to 1.5 time H-mode and two to three times L-mode. One may add here that a fraction of the stored energy is contained in the non-thermal ions (≈ 25 – 30 %), but that roughly the same amount of NBI power is lost through charge exchange and bad orbits. Another paper at this conference discusses NSTX's NBI driven H-mode plasmas in detail [6].

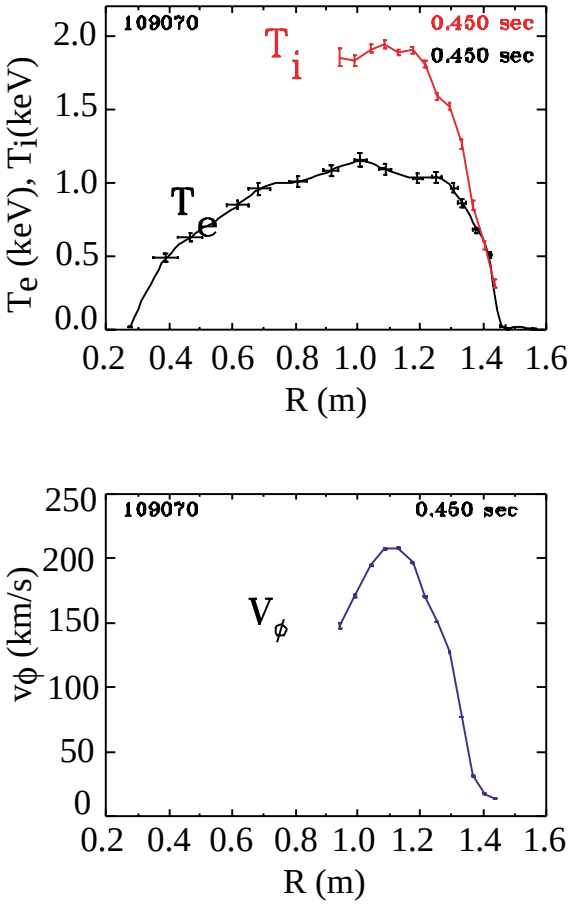

FIG 2: Profile of Te and Ti during high NBI power (a). Toroidal velocity profile (b).

3. Kinetic Documentation of Analysis

An important development during the last two years has been the coming on line of baseline profile diagnostics like Thomson scattering for $n_e(R,T)$ and $T_e(R,t)$, charge exchange recombination spectroscopy for the measurement of $T_i(R,t)$ and toroidal velocity $v_\Phi(R,T)$ and bolometry for radiated power $P_{rad}(R,t)$. The availability of profile and temporal information has permitted the use of

the TRANSP [7] code to establish a consistency check of the kinetic data set with respect to global measurements, and also to begin investigating local transport through power balance calculations. One limitation remains that, for the moment, we do not have a routine profile measurement of Z-effective, and we typically have to rely on a single chordal measurement which gives a time history of the line-average Z-effective. Details about the NSTX diagnostic data set can be found elsewhere [8].

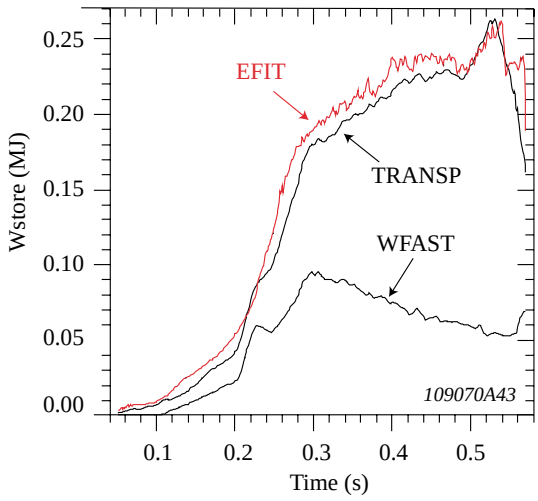

FIG. 3(a): Temporal overlay of the measured stored energy and TRANSP estimate. TRANSP reproduces well the measured stored energy.

Shown in Fig. 2(a) is an overlay of the experimental T_i and T_e profiles obtained during a high power (6 MW) H-mode discharge. A good match between T_i and T_e is seen in the edge region, as to be expected in this collisional region of the plasma. In some discharges, $T_e > T_i$ in this region. A substantial difference is observed in the central region, where T_i=1.9 keV while T_e = 1.1 keV. Since the NBI system uses beam energy typically around 80 keV, which is many times larger than the typical 1-2 keV electron temperature, one would expect from classical slowing down physics of fast particles that most of the neutral beam power be deposited into the electron population. The repeated experimental observation that T_i is greater than T_e during NBI despite the preferential electron heating suggests that the ion confinement is much better than that of the electrons.

The measured kinetic profiles reproduce well global measured parameters such as the displaced magnetic flux, the neutron production rate and the stored energy as determined from EFIT reconstructions. In Fig. 3(a) is shown an overlay of the TRANSP temporal estimate of the stored energy compared to that from EFIT [9]. The good match seen throughout the time evolution indicates agreement between magnetic and kinetic estimates of the stored energy. A similar comparison for the neutron production rate is shown in Fig. 3(b). The TRANSP estimate, based on the Monte-Carlo neutral beam deposition calculation, is compared to fission-chamber measurement. The experimental error-bar extent of ±25% reflects the fact that this diagnostic was recently installed, and is expected to be reduced as neutron calibration work progresses. Large scale MHD activity developed in this discharge at 0.48 sec. The discrepancy between the measured and calculated neutron signal after this time indicates that fast ions are either expelled or

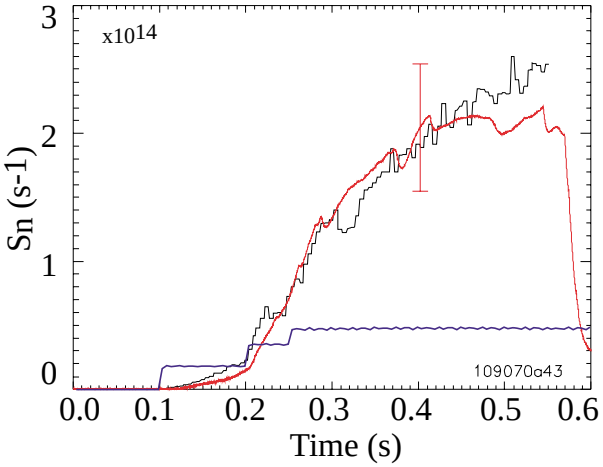

FIG. 3(b): Temporal overlay of the measured neutron rate and TRANSP estimate. TRANSP reproduces well the measured DD neutrons.

redistributed by the MHD. This loss/redistribution has not yet been modeled, but the agreement between the TRANSP and EFIT calculated stored energies through the MHD active period, along with the neutron signal discrepancies, will set an bound on the magnitude of this effect.

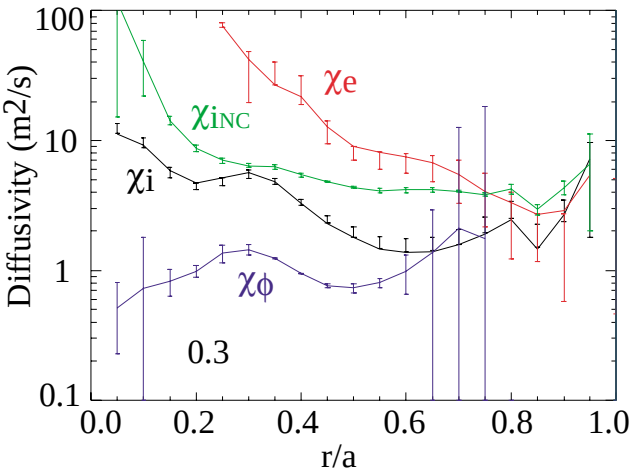

FIG. 4: Diffusivity profiles: electron thermal χ_e, ion thermal χ_i, ion neoclassical χ_{inc} and momentum χ_ϕ. Error bars represent range of TRANSP analyses.

Fig 4 shows profiles of the power and momentum balance diffusivities obtained at 0. 45 s, corresponding to Fig. 2. χ_i is close to the neoclassical level as determined by NCLASS [9]. An error bar analysis based on the error in measurements is likely to bridge the gap between χ_i and $\chi_{i,nc}$, although such work has not been done so far. The neoclassical ion diffusivity is computed with the NCLASS code [10]. The momentum diffusivity is lower than the thermal diffusivities, reaching tokamak-like levels of 1 m^2/s in the core region. On the other hand the electron thermal confinement is poor, with χ_e values that can exceed 10 m^2/s, reflecting the flat core T_e profile seen in Fig. 2. These results support the inference that the ion confinement is superior to that of the electrons in the NSTX NBI discharges. A preliminary microinstability analysis using the gyrokinetic code GS2 [11] indicates that the ITG drift modes are stable in the extended core region ($r/a \leq 0.6$), whereas the ETG drift modes are found to be unstable across most of the plasma.

4. Perturbative Transport Measurement

The ion particle transport was probed in an experiment where small amount of neon ($n_{neon}/ne \approx 0.5\%$) was injected for 20 msec during non H-mode discharges. Using two ultrasoft x-ray diode arrays [12] fitted with Be foil filters having respectively 0.6 keV and 1.4 keV cutoff energy, radiation emitted from the peripheral and core charge states was measured simultaneously. The local emissivity was obtained by inverting the SXR signals, and it is

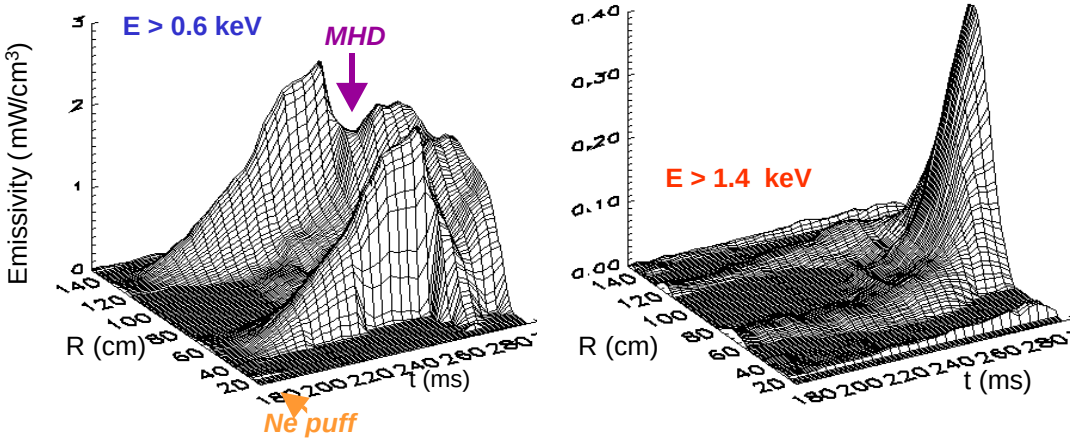

FIG. 5: Local emissivity reconstruction against time for the two USRX energy ranges. Radiation is contained to within the peripheral region until MHD reconnection.

displayed in Fig. 5 for the two energy ranges. The radiation from the lower neon charge states range was emitted from the peripheral region following the gas puff, while essentially no radiation came from the core region. Only when an MHD reconnection occurred at $t \approx 0.26$ s, did the peripheral radiation collapse and was radiation emitted from the core region, indicating that neon does not penetrate beyond $r/a \approx 0.5$-0.6. By modeling the instrumental emission and making use of the MIST impurity transport code [13], a particle diffusivity profile can be obtained; this diffusivity is found to in the range of NCLASS neoclassical prediction for low-Z impurities in the extended core area, consistent with the power balance results. Figure 6 overlays the experimental results and the neoclassical prediction for carbon.

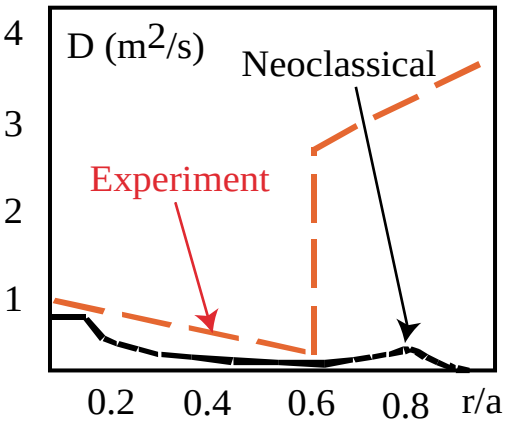

FIG. 6: Experimentally derived particles diffusivity and neoclassical prediction.

5. HHFW Driven H-mode Discharges

High Harmonic Fast Wave (HHFW) heating and current drive is a major component of the NSTX research program. Electron heating with HHFW can be effective; under some conditions, central electron temperatures in the 3-4 keV range were obtained. Transitions into the H-mode were observed with HHFW heating only, and the relevant parameters for such a discharge are shown in Fig. 7. The plasma current was 0.36 MA, and the magnetic field was 0.45 T. HHFW power of 3.3 MW was applied during the interval from 0.12-0.32 s. The HHFW frequency was 30 MHz and the launched spectrum was centered around 14 m^{-1}, the nominal mode of operation for isotropic electron heating. T_{e0} rapidly responded to the HHFW heating by increasing from 0.3 keV to nearly 1.5 keV in 0.05 s. The L-H transition occurred at 0.195 s and was accompanied by a further heating of the electrons and an increase in the stored energy. The decrease in central electron temperature observed later in the pulse probably resulted from a power coupling loss caused by MHD activity or the ELMs (visible on the Dα trace). On other occasions, peaked electron temperatures can be maintained during the ELM activity as illustrated in Fig. 8. In this case, T_e remained above 1.5 keV for 0.1 s, including times of ELM activity. Maintaining good coupling during HHFW H-mode

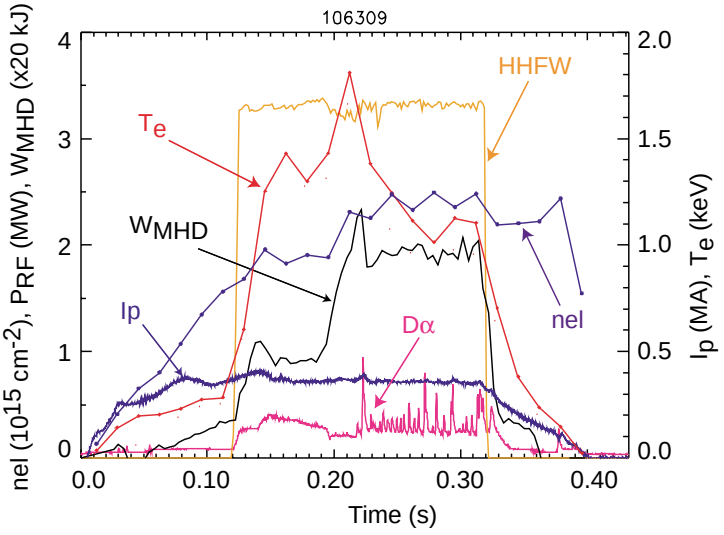

FIG. 7: Time evolution of HHFW driven H-mode discharge. The transition and ELMs are seen on the Dα trace. The stored energy doubles after the transition.

discharges was found to be a challenging task, either because of the rapidly changing edge density or ELM activity. We can see in Fig. 9 T_e and n_e profiles for two discharges. One was heated with HHFW and the other is a reference discharge. Both discharges had identical beam blips for T_i measurement. The application of 3 MW of HHFW power started at t = 0.1 s for the discharge shown in red. The reference discharge is shown in dotted black. The profiles shown in Fig. 9 were measured at t = 0.193 *s*. In NSTX, ohmicly heated discharges typically have a peaked density profile as seen for the reference discharge. The situation is quite different for the HHFW heated plasma, where we can see that $n_e(R)$ has developed – from a peaked profile – to a flat profile with "shoulders" near the peripheral region, and large density gradient at the edge, typical of NSTX H mode. After the onset of the H mode, the line integrated density doubled from 1.9 x 10^{19} m^{-2} to 3.8 x 10^{19} m^{-2}. The T_e profile has developed a pedestal in the edge region, and is centrally peaked in response to the HHFW electron heating. The central T_e is 60% greater than for the reference plasma.

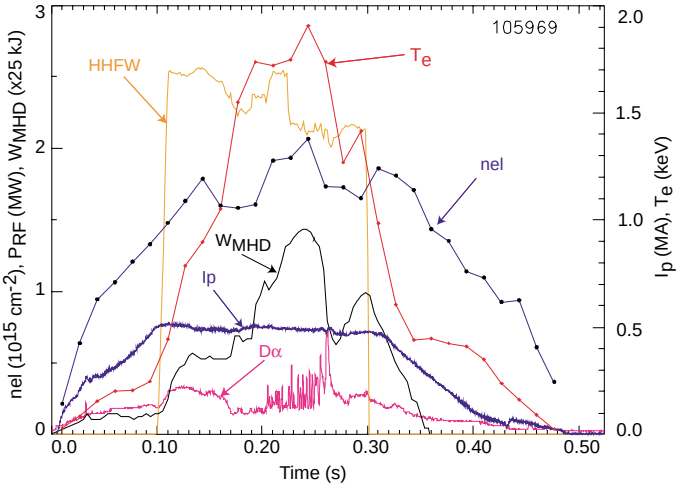

FIG. 8: Time evolution of HHFW driven H-mode discharge. The transition occurs at 0.16 s. Elm activity starts at 0.21 s. Stored energy and T_e increase is maintained during H-mode phase.

6. Conclusion

The energy confinement of NSTX plasmas is seen to be enhanced over the values given by both L-(ITER97L) and H-mode (ITER09Pby(2)) scalings, being respectively up to two to three times L-mode and up to 1.5 times H-mode. L-mode edge plasmas have energy confinement times comparable to those of H-mode discharges. Measured global parameters such as diamagnetic flux and neutron rate agree with those determined from TRANSP calculations based on the measured kinetic profile data. This transport analyses give power and momentum balances which appear different than what is usually seen in tokamaks. The ion thermal diffusivity can be near neoclassical level over a wide region of the plasma, for instance. The momentum diffusivity appears lower than χ_i, reaching tokamak-like levels. The particle diffusivity is estimated to be also at neoclassical

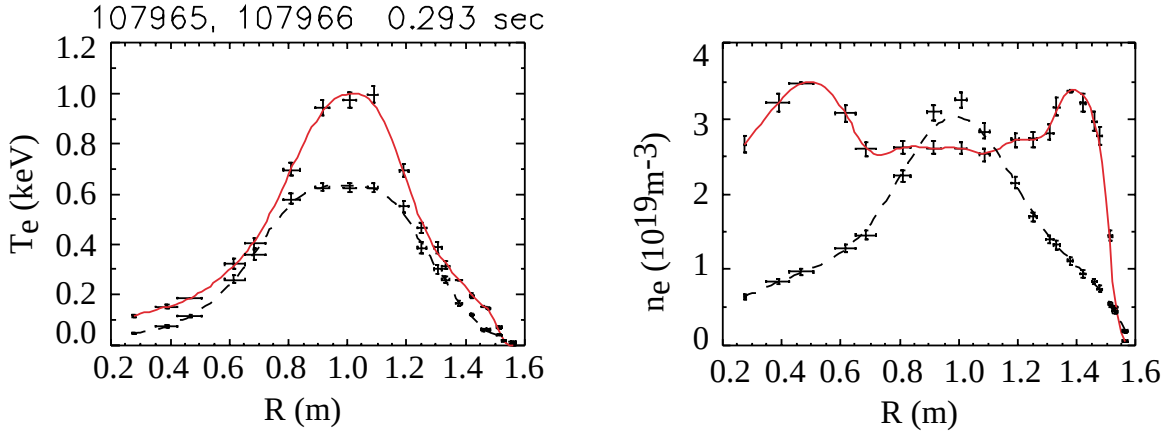

FIG. 9: $T_e(R)$ and $n_e(R)$ profiles for a HHFW heated discharge during H-mode phase, in solid red, and for a reference discharge without RF power, in dotted black.

level in the core region of L-mode discharges based on results from a neon-puff experiment. The electron thermal transport is found to be much larger than for the thermal ions. The themal and momentum diffusivities presented here correspond to a limited set of the NSTX experimental data. NSTX has obtained H-mode discharges during HHFW heating. The latter results puts NSTX in a good position to study the physics of the H-mode transition and the role of rotation by comparing NBI driven and HHFW driven discharges.

This work is supported by U.S. DOE contract DE-AC02-76CH03073.

[1] Y. –K. PENG, Phys. Plasmas 7, 1681(2000)
[2] J.E. MENARD et al, paper IAEA-CN-94/EX/S1-5 at this conference.
[3] C. H. SKINNER, et al. Nucl. Fusion **42**, (2002) 329.
[4] S.M. KAYE and the ITER CONFINEMENT DATABASE WORKING GROUP, Nucl. Fusion, **37** (1997) 1303
[5] ITER PHYSICS, Nucl. Fusion, **39** (1999), 2175
[6] R. MAINGI, et al., paper. IAEA-CN-94/EX/C2-5 at this conference.
[7] J. ONGENA, M. EVRARD, D. MCCUNE, "Numerical Transport Codes", in the Proceedings of the Third Carolus Magnus Summer School on Plasma Physics, (Spa, Belgium, Sept 1997), as published in Transactions of Fusion Technology,
March, 1998, Vol. 33, No. 2T, pp. 181-191.
[8] DW JOHNSON et al., German-Polish EURO-Conference on Plasma Diagnostics for Fusion and Applications, Greifswald, Germany, September 4-6, 2002
[9] S. A. SABBAGH, S. M. KAYE, J. MENARD, et al., Nuclear Fusion 41 (2001)
1601.
[10] M. R. WADE, W. A. HOULBERG and L.R. BAYLOR, Phys. Rev. Lett. 84, 282(2000)
[11] M. KOTSCHENREUTHER, G. REWOLDT and W.M. TANG, Computer Phys. Com. 88, 128 (1995).
[12] D. STUTMAN, M. FINKENTHAL, C. BOURDELLE, et al, Proc. of 29th Euro. Conf. on Plasma Physics and Contr. Fusion, Montreux, Switzerland, June, 2002, paper P4.067.
[13] R.A. HULSE, Nuclear Technology/Science 3, 259 (1983)